The following document is a pre-print version of:

Graettinger AH, Valentine GA, Sonder I, Ross P-S, White JDL (2015) Facies distribution of ejecta in analog tephra rings from experiments with single and multiple subsurface explosions. Bull. Volc. 77:Article 66

Facies distribution of ejecta in analog tephra rings from experiments with single and multiple subsurface explosions

Graettinger, A. H.[1]; Valentine, G.A. [1]; Sonder, I. [1]; Ross, P.-S.[2]; White, J.D.L.[3]
1. Department of Geology and Center for Geohazards Studies, 411 Cooke Hall, Buffalo, NY 14260, State University of New York, USA
2. Institut National de la Recherche Scientifique, Centre Eau Terre Environnement, 490 rue de la Couronne, Québec, Québec, G1K 9A9 Canada
3. Geology Department, University of Otago, P.O Box 56 Dunedin 9054, New Zealand

Keywords: ejecta; tephra ring; discrete explosion; proximal deposits

Corresponding author: agraettinger@gmail.com

Abstract
The volume, grain size, and depositional facies of material deposited outside an explosion crater, ejecta, are sensitive to the depth of the explosion, the explosion energy, and the presence or absence of a crater before the explosion. We detonate buried chemical explosives as an analog for discrete volcanic explosions in experiments to identify unique characteristics of proximal, medial and distal ejecta facies and their distribution from a range of scaled depths in undisturbed and cratered ground. Ejecta are here discussed in terms of three facies: (1) proximal ejecta, which form a constructional landform around a crater; (2) medial ejecta, which form a continuous sheet deposit that thins much more gradually with distance; and (3) distal ejecta that are deposited as isolated clasts. The extent of proximal ejecta away from the crater, relative to crater size, is not sensitive to scaled depth, but the volume proportion of proximal ejecta to the total ejecta deposit is sensitive to the presence of a crater and scaled depth. Medial ejecta distribution and volume contributions are both sensitive to the presence of a crater and to scaled depth. Distal ejecta distance is dependent on scaled depth and the presence of a crater, while the volume proportion of distal ejecta is less sensitive to scaled depth or presence of a crater. Experimental facies and deposit structures inferred from observations of jet dynamics are used to suggest facies associations anticipated from eruptions dominated by explosions of different scaled depth configurations. We emphasize that significant differences in tephra ring deposits can result from the effects of scaled depth and preexisting craters on ejecta dynamics, and are not necessarily related to fundamental differences in explosion mechanisms or degree of magma fragmentation.

1. Introduction

Discrete explosions at volcanoes can occur in isolation or as part of a longer eruptive sequence through a range of processes such as hydrothermal explosions (Browne and Lawless 2001; Ruapehu 2007: Kilgour et al. 2010; Te Maari 2012: Breard et al. 2014), littoral explosions (Mattox and Mangan 1997); bubble-driven bursts (Strombolian jets: e.g., Taddeucci et al. 2012; Harris et al. 2012; Gurioli et al. 2013), external perturbation of a lava lake (Halemaumau 2008- present: Swanson et al. 2009; Houghton et al. 2011; Carey et al. 2012) and phreatomagmatic explosions (Ukinrek Maar 1977: Self et al. 1980). The jets produced by these explosions can contain particles with a wide range of sizes and in varied concentrations, and occur individually or as products of one of tens or hundreds of explosions in a sequence. Extra-crater (i.e. ejecta, or tephra) deposits from these explosions, including the dispersal of materials originating from different depths in the subsurface, are related to characteristics of the explosions, but little work has been done to unravel this relation.

Analog experiments involving subsurface explosions in granular media have been used to test

relations between explosion energy and resulting surface and subsurface structures of single (referred to here as primary) and multiple explosion experiments (Ross et al. 2013; Andrews et al. 2014; Graettinger et al. 2014). Similar experiments using compressed air and glass beads have looked at subsurface structures during formation in two dimensions (Ross et al. 2008a, 2008b; Andrews et al. 2014). These tests have supported important relations, first reported in the military and geotechnical literature, between the scaled depth and whether or not a subsurface explosion will produce an eruptive jet or remain confined to the subsurface (Valentine et al. 2014). The explosion experiments have produced a growing dataset of well-characterized surface deposits. These data are used here to investigate relations between the distribution of extra-crater deposits (here termed ejecta) and the energy and depth of the explosion that produced them as well as the influences of pre-existing craters. The role of the pre-explosion crater also influences ejecta componentry as influenced by subsurface mixing and material that was transported by previous explosion jets but that did not escape the crater, referred to here as fallback. This study does not aim to comment on different explosion mechanisms within these systems, but rather on the effects of an explosion within debris-filled systems like diatremes, regardless of explosion mechanism. We present descriptions of experimental deposits and relate them to facies that are observed in tephra rings at maar-diatreme volcanoes.

2. Approach

Experiments were conducted to investigate the relations between explosion energy, depth of burial and multiple explosions on the resulting subsurface and surface structures, with particular focus on applications to maar-diatreme eruptions (Valentine et al. 2012). The experimental structure involves buried chemical explosives in constructed stratigraphy of readily available geomaterials to produce craters 1-2 m in diameter and disperse ejecta up to 30 m from the explosion site. The experiments were conducted in four sets with variable conditions (layer thickness, ordering of geomaterial layers, charge size and burial depth and numbers and locations of explosive charges). Geomaterials used included poorly-sorted angular limestone sand, lithic-rich rounded sand and recycled asphalt product in compacted layers between 15 and 75 cm thick. Explosive charges were *PENTEX*™ boosters made of a combination of PETN (pentaerythritol tetranitrate) and TNT (trinitrotoluene) with energies ranging from 7.5×10^5 to 2.3×10^6 J. Charges were buried between 0.1 and 1 m below the ground surface in both undisturbed geomaterials and in craters produced by previous explosions with between one and four explosions at the same plan-view position.

The relation between energy and depth of explosion can be characterized by one parameter, scaled depth:

$SD = d / E^{1/3}$

Where d is depth (m) and E is the energy (J) of the explosion. Depth to the explosion is always measured to existing surface. For a given explosion location (depth), scaled depth will decrease if energy is increased, resulting in apparent shallower behavior. For the same depth, scaled depth will increase with decreasing energy, which results in a larger (deeper) scaled depth value. For undisturbed ground depth is relative to flat ground, and for explosions through craters it is relative to the crater bottom. For purposes of comparison, we refer to the optimal scaled depth (OSD), the condition in which the largest craters are produced, which is ~0.004 $m/J^{1/3}$ (e.g. Goto et al. 2001). For larger or smaller scaled depths, the scaled crater will be smaller. Those scaled depths smaller (shallower) than optimal produce large jets (in experiments: 15-25 m tall). Explosions that occur at scaled depths greater than optimal produce much smaller jets (in experiments: 0.5-10 m). At scaled depths of ~0.008 $m/J^{1/3}$ and greater, explosion energy is predominantly confined to the subsurface, and does not produce jets or ejecta (Valentine et al. 2014).

Ejecta were collected in sample boxes at 1 m increments along two 18 m arrays, radial from the explosion epicenter and separated by >45°. The first sample box was placed at either 1.5 m or 2 m from the epicenter to avoid interference with crater formation. The mass loading (mass per unit area) as a function of radial distance was calculated for each explosion for the two arrays. The mass loading had some variability between the two arrays, reflecting heterogeneity in the jets that produce rays of higher concentrations of ejecta in the deposit (Graettinger et al. 2014). In this discussion, we use the average of the two arrays. Additionally, the components of the ejecta were investigated by Graettinger et al. (2014) to identify the depth of origin of materials within the fallback and ejecta. More detailed descriptions of experimental setups can be found in Valentine et al. (2012) and Graettinger et al. (2014).

As a result of the scale of the experiments and the low proportion of fines in the materials used, the jets did not become buoyant, and only a small mass proportion of the particles lofted in a gas-particle suspension. The main jet collapsed in two main styles. For explosion energy and depth combinations that are near the optimal scaled depth, the ejected mixture followed ballistic trajectories that formed an outward advancing front. We refer to this as a ballistic curtain, a term used in the meteorite impact community (e.g. Melosh 1989). Ballistic curtain deposits tend to be poorly sorted, including both fine and coarse grained material, and be massive in structure (Melosh 1989 and

this study). The ballistic curtain mechanism dominated proximal and medial deposition in these experiments, whereas distal deposits were mainly composed of individual clasts that travelled along independent ballistic trajectories (Fig. 1a; video Online Resource 1). In contrast, density currents of fine particles mixed with air were observed during explosions at large scaled depths through pre-existing craters. The currents are produced by the expulsion of fine particles and air by the collapse of the vertically focused explosion jet back into the crater (Fig. 1b; video Online Resource 2). The density currents produced by the experiments were dilute and did not leave identifiable and measurable deposits (Graettinger et al. 2014), but natural volcanic explosions may involve larger proportions of fine particles and result in appreciable density-current-emplaced ash deposits (e.g. maar and hydrothermal explosion tephra rings; White and Ross 2011; Breard et al. 2014; Lube et al. 2014). The masses of the experimental deposits are $5x10^2$-$1x10^3$ kg, which are from subequal to two orders of magnitude smaller than the deposits of natural volcanic events (8×10^2 kg small Strombolian bursts, Ripepe et al. 1993) and five orders of magnitude smaller than those to which they are being compared ($5x10^8$ kg Ruapehu 2007, Kilgour et al. 2010; ~10^8 kg TeMaari, Lube et al. 2014). Based on the ejecta volumes the 'eruptions' produced in these studies would be considered a VEI -6 by the extended VEI scale, proposed by Houghton et al. (2013) to include small eruptions.

The ejecta of the explosion experiments can be divided into three facies -- proximal, medial and distal (Graettinger et al., 2014) -- based on the morphology of the deposits (Fig. 1c). The proximal ejecta formed a constructional feature similar to a tephra ring around each crater. The limit of the proximal deposits is defined here as the radius where the outer slope of the crater rim changes from values that exceed 20° to slopes that average <10°. Proximal deposit volumes were calculated from 1-cm-resolution digital elevation models (DEMs) produced from photogrammetry of the craters. The DEMs were derived from point clouds produced in *AgiSoft*© software from ~15-30 images, and processed in *ArcGIS*. Volume calculations of the proximal ejecta used the Surface Volume tool in 3D Analyst for all material above the original surface to the edge of the proximal facies ring. Proximal deposit volumes for individual deposits were based on the change in volume of that deposit from the previous surface.

Medial ejecta consisted of continuous sheets that mantled existing topography. Many experiments showed ray-like structures that produced local deposit asymmetry; consequently, for this study an average of two sample box arrays were used to account for this variability. Distal ejecta were deposited as isolated clasts. A mass loading of 0.1 kg/m^2 was used to define the transition between medial and distal ejecta. The volumes of medial and distal ejecta were calculated using the mass loading from each sample over an isopach area defined from the location of the samples. This incremental volume is probably a minimum estimate.

Twenty-eight explosions from the experimental dataset are investigated here, out of which seventeen produced large ejecta deposits. Of these, fourteen were explosions in undisturbed geomaterials with flat surfaces, and fourteen explosions occurred beneath previous craters. With the exception of one explosion, all proximal deposits occurred within 2 m of the explosion epicenter and did not reach the sample boxes. Medial and distal deposits produced at multi-blast sites were collected for each individual explosion and were assessed independently. Qualitative observations of experiments that produced smaller deposits (particularly for explosions deeper than OSD) are included in the discussion and detailed descriptions of these experiments can be found in Graettinger et al. (2014) and Valentine et al. (2015).

3. Lateral extents of proximal, medial and distal facies

We follow the precedent of the military and meteorite impact literature and discuss ejecta distribution in terms of the dimensionless ratio of distance (deposit distance: D_{dist}) to crater radius (C_R; i.e. Housen et al. 1983). Ejecta from the 28 explosions extended 0-20 m away from the explosion epicenter or roughly 24 times the crater radius for maximum deposit extent (0-24 C_R), producing proximal, medial and isolated distal ejecta. The greatest radius of the proximal ejecta facies did not exceed two times the crater radius (2 C_R; Fig. 2a). The mass loading of the medial facies typically exceeded 5 kg/m^2 up to 4 m from the explosion center (4-6 C_R), and rapidly decayed with distance. Several explosions had near-crater mass loading of medial ejecta as high as 15 kg/m^2, which then decayed rapidly with distance. The maximum distance ejecta travelled from any given explosion generally increased with decreasing scaled depth for both primary and multi-blast experiments (Fig. 2b). As proximal ejecta distance was not sensitive to scaled depth, a ratio between proximal ejecta distance (P_R) and maximum distal ejecta distance, P_R/D_{dist}, shows that the data fall within an envelope, wherein the maximum ratio decreases with decreasing scaled depth (Fig. 2c).

High-speed video of the explosions reveals that maximum jet height ($\leq 27\ C_R$) increases with decreasing scaled depth (Fig. 2d), supporting observations of a smaller dataset by Graettinger et al. (2014). Multi-blast experiments produce a similar trend for all but the lowest scaled depths (<0.002 m/J$^{1/3}$). The data plotted in

Figures 2b and d indicate that maximum ejecta distances correspond with maximum jet heights, but are complicated by the presence of a crater. This is simply because shallow-scaled-depth explosions launch particles on a wide range of ballistic paths, while those at deeper-than-optimal scaled depths and those beneath craters produce lower and vertically focused jets with a narrow range of launch angles (Ohba et al. 2002; Taddeucci et al. 2013; Graettinger et al. 2014). Conversely, explosions through hummocky crater fill or a retarc (positive topographic feature) produced jets with very wide jet angles (Valentine et al. 2012; Graettinger et al. 2014). For all large scaled depths, most material is deposited close to the crater or even in it, as fallback.

Explosions from OSD, and some explosions shallower than OSD, commonly produced clumps of loosely aggregated sands and gravels that were thrown up to 13 m from the explosion site, producing local increases in mass loading. Clumps were most common within seven meters of the explosion center (<9 C_R). The clumps were typically disaggregated on impact and thus could not be measured for size or density, but were estimated to be up to 10 cm in diameter from high-speed video data.

4. Volume proportions of proximal, medial and distal facies

The volumes of ejecta in proximal, medial and distal facies were compared for each explosion against conditions of scaled depth and ground surface (flat or with pre-existing crater) prior to explosion. The largest total volumes of ejecta were produced at OSD conditions and decreased for both decreasing and increasing scaled depths away from OSD (Fig. 3a). No discernable ejecta were produced from scaled depths greater than 0.008 m/$J^{1/3}$ (Valentine et al. 2014). In all of these experiments, proximal deposits provide an important contribution, 60-90% for multi-blast systems and 5-90% in primary explosion systems, to the overall deposit volume (Fig. 3). Eruptions through craters yielded deposits with the greatest proportions of ejecta in the proximal facies because jet focusing limited the distance of ejecta distribution (Taddeucci et al. 2013; Graettinger et al. 2014). The volume proportion of distal ejecta was not sensitive to scaled depth or the presence of a crater and was always less than 10% of the total deposit volume. Consequently, the following discussion occasionally treats medial and distal ejecta together.

4.1 Primary explosion experiments

The volume of ejecta produced by primary explosions increased as depths were reduced from deeper than OSD ones; the volume peaked at OSD (ca. 0.8 m^3) and then decreased as scaled depth decreased (Fig. 3a; Table Online Resource 3). The range of volumes for primary explosion experiments was 0.1-0.8 m^3. The absolute volumes of the three facies display some correlation with scaled depth, but the maximum volumes of medial and distal ejecta do not correlate with the explosions that produced the most proximal ejecta. All three facies have high volumes at OSD with frequently smaller absolute volumes of ejecta for explosions of depths both lower and higher than OSD. The distribution of volume between proximal and medial + distal facies of experimental explosions was more revealing (Fig. 3b-c). The volume proportion of proximal deposits decreased with decreasing scaled depth in primary explosions through flat ground, contributing from 90% at deeper than OSD to <10% of deposit volume for shallower than OSD explosions (Fig. 3b). At OSD conditions, the proportion of proximal deposits ranged from 25-75% of ejecta volume. Conversely, medial ejecta facies contributed progressively more volume to the total deposit as scaled depth decreased from OSD (55-93%).The volume proportion of distal ejecta remained consistent for all scaled depth conditions (5-10 % vol.; Fig. 3d). These single explosions through undisturbed ground likely shed light on the initiation of maar craters, and they resembled examples from the military blast and impact literature. The bulk of deposits known from natural tephra rings will be the product of explosions through pre-existing crater structures due numerous explosions represented in the many beds of tephra rings and the limited exposure of the initial primary deposits. Consequently, multi-blast experiments will be the focus of the remainder of the discussion.

4.2 Multi-blast experiments

Multi-blast experiments produced a wider range of ejecta volumes, but the values fell within the envelope of total volumes produced by primary explosions with the greatest total volumes produced by OSD and shallower-than-OSD explosions (> 0.3 m^3; Fig. 3a). Craters resulting from two or more explosions had more proximal ejecta and less medial or distal ejecta for scaled depths <0.005 m/$J^{1/3}$, compared to primary explosion experiments (Fig. 3b).The volume fraction of proximal deposits in multi-blast systems was high (~90% vol.) for all but OSD (~60% vol.) explosions (Fig. 3c,d). This contrasts with the trend of primary explosions for shallower-than-OSD conditions and is a direct result of the presence of a crater, which focused the jet and results in a narrower distribution of ejecta despite increased jet height.

The multiple explosion system showed further complexity in the experiments that involved three or more explosions. The condition of a crater, presence of fallback, and stability of crater walls were dependent on the explosion itself. Consequently, behavior of any explosion through a cratered system was influenced by

the previous explosion(s). For the experiments conducted here, a shallow-scaled-depth explosion that followed an optimal-scaled-depth blast (e.g. 2013bP1B1 in the table Online Resource 3) produced a smaller volume of ejecta than would be predicted from scaled depth alone. This is inferred to be a direct reflection of the volume of fallback returned to the crater by the preceding blast, which results in a greater distance from the crater floor to the crater rim (crater depth) and a smaller volume of highly disrupted material above the explosive. That is, when the volume of fallback from a given explosion is limited, the subsequent explosion at the same position is more affected by focusing of the crater. Shallow-scaled-depth explosions are probably more sensitive to surface crater conditions than are those at greater-than-optimal scaled depths.

5. Discussion

5.1 Effect of scaled depth and pre-existing crater on ejecta distribution

The capacity for an explosion to create ejecta by removing material from the crater, and the partitioning of ejecta volume among the three depositional facies depends on scaled depth and the presence of a pre-existing crater for the same explosion mechanism. Scaled depth is a measure for the potential energy (confinement) that must be overcome by an explosion. This is strongly controlled by the mass of material above the explosion location. For all explosions that produced a jet, material was divided between the ejecta (extra-crater deposits) and fallback (material that returned to the crater). All blasts that formed a jet also produced fallback. For shallower-than-optimal scaled depth explosions, much of the explosions' energy was lost to the atmosphere, but the explosions could still distribute distal ejecta to great distances. A shallow explosion has less material available above the explosion, which reduces the total ejecta volume. There is also less inertia acting against the expanding explosion gases, so a small volume fraction of the ejected material (<10%) can be accelerated and ejected from the epicenter to distances as far as 24 times the crater radius (distal ejecta). The bulk of the ejecta, however, is poorly coupled to these shallow-sourced jets and is deposited in the crater or on the rim as proximal ejecta. As scaled depth increases toward optimal conditions, the mass above the explosion site, for a given explosion size, increases and the jet also more effectively couples with the overlying material, transporting more of it out of the crater to produce a significant medial ejecta blanket, in addition to isolated clasts of distal ejecta, a proximal ring, and fallback deposits.

At depths greater than optimal, the results change dramatically. Deeper explosions produce small jets that result in limited ejecta. The ejecta that is produced forms a proximal ring, while the bulk of the lofted material returns to the crater as fallback. The small proportion of material that is ejected beyond the proximal ring is limited in volume and distance; it mostly forms distal facies (i.e. patchy, discontinuous) deposits close to the crater. For explosions at sufficiently large scaled depths, greater than ~ 0.008 $m/J^{1/3}$, the potential energy of the overlying mass is not overcome by the explosion energy. It instead mixes the subsurface materials and contributes to subcrater structures that resemble diatremes under maar volcanoes (Ross and White 2008; Ross et al. 2013; Graettinger et al. 2014; Valentine et al. 2015). These contained explosions produce no extra-crater ejecta. Subsidence produces a collapse pit in some experiments (Valentine et al. 2014).

The presence of a crater before an explosion influences jet shape (Taddeucci et al. 2013; Graettinger et al. 2014) and here this influence is revealed in the production of proximal deposits. For shallower-than-optimal-scaled-depth explosions through existing craters, the volume proportion of proximal deposits is typically higher than would be produced by a similar scaled depth beneath flat ground. This is because the crater walls limit the initial lateral expansion of the jet and thus the ability of the jet to launch particles on a wide range of ballistic angles. Similarly, explosions through a crater produce less distal ejecta than would be produced by a similar-scaled-depth explosion beneath flat ground (Fig. 3b and d).

The general results of the experiments with respect to facies distribution can be summarized as follows (Fig. 4). Primary explosions beneath flat ground tend to have increasing proportions of proximal ejecta, relative to medial and distal ejecta, with increasing scaled depth up to values of ~0.0055 $m/J^{1/3}$ (Fig. 4a). At deeper scaled depths, there are negligible medial and distal ejecta, and proximal ejecta deposits and fallback dominate. At scaled depths great than ~0.008 $m/J^{1/3}$ explosions are fully contained. In contrast, explosions beneath pre-existing craters produce appreciable medial and distal deposits only when the scaled depth is at, or close to, the optimal value of ~0.004 $m/J^{1/3}$ (Fig. 4b). Such near-optimal-scaled-depth explosions have sufficient energy coupling with, and lofting of, the overburden to partly overcome the confining effects of the crater walls and disperse material beyond them on a range of ballistic paths. Optimal-scaled-depth explosions below small preexisting craters will excavate a new crater, and therefore do not experience jet focusing. At shallower scaled depths, there is little coupling of energy into host material and the resulting jet is subject to focusing by the crater walls. At deeper scaled depths, the amount of host material above the explosion reduces its lofting potential and vertical focusing of the jet reduces dispersal beyond proximal deposits. To summarize, optimal-scaled-depth

explosions produce significant volumes of medial and distal ejecta for both primary and multi-blast craters (Fig. 4). Explosions deeper than optimal scaled depth behave similarly for undisturbed and cratered conditions in that proximal ejecta dominate the deposits, comprising at least 90% of the total volume, which is contained within two crater radii of the explosion.

In a primary explosion experiment, the material that hosts the explosion is structured, in this case consisting of layered and mechanically compacted sands and gravels. In multi-blast craters, the available material is deposits from preceding blasts and consist of fallback, slumped crater rim materials and subcrater material (Ross et al. 2013; Graettinger et al. 2014), plus, for greater scaled depths, possible undisturbed host material. Exactly which materials are available above an explosion depends on the sequence of previous explosions (size, number and location). Some greater-than-optimal-scaled-depth explosions produced abundant fallback that resulted in positive topography, known as a retarc (Graettinger et al. 2014). This feature provides abundant disrupted material at the epicenter above sites of future explosions, which consequently have very wide jet angles. Retarc-like features may form in natural maar-diatreme systems, but are likely to be ephemeral.

Multiple explosion experiments enable the consideration of the importance of the sequence of a series of variable-scaled-depth explosions (Fig. 5). Where the scaled depth relative to crater bottom remains constant as a crater deepens (as might be anticipated in a system experiencing systematic explosion deepening due to groundwater drawdown as envisaged by Lorenz 1986), the volume proportion of proximal ejecta increases at the expense of medial and distal facies. The proportion of the jet that returns to the crater as fallback also increases as the crater focuses the jet and reduces the range of ballistic ejection angles. Consequently, maintaining a constant scaled depth does not result in simply increasing crater depth. As the total depth relative to the crater rim increases, the total volume of ejecta (material escaping the crater) would decrease as the travel distance to escape the crater approaches the jet height and the crater walls focus the jets to reduce the range of ballistic ejection angles. This trend would be amplified if a system has experienced any crater widening resulting from lateral migration of the explosion location or slumping or collapse of the crater rim, increasing the travel distance to the ejecta ring (Carrasco-Nuñez et al. 2007; Ort and Carrasco-Nuñez 2009; Jordan et al. 2013). If the scaled depth decreases (progressively shallower explosions with constant energy, or steady location with increasing explosion sizes), the total volume of ejecta increases where scaled depth is initially high (larger than optimum) and where crater sizes were initially small. These explosions then excavate beyond the the previous crater and reduce the focusing effect of the topography. Instances of increasing scaled depth for explosions beneath a crater have not yet been tested, but the increase in relative mass above the explosion would be expected to absorb a greater portion of the energy and reduce the jet height, and therefore ejecta distribution. For systems that experience multiple explosions, progressively increasing scaled depth would likely decrease the total volume of ejecta while increasing the proportion deposited proximally, eventually reaching the depth threshold beyond which explosions are fully confined.

The presence of a crater and disrupted host material also influences how host material components, originating at different depths, are distributed in the ejecta (Fig. 6; Graettinger et al. 2014). For shallower-than-optimal and optimal-scaled-depth explosions, material located immediately above and at the same level as the explosion is incorporated into the fallback, but rarely is present in the ejecta. Greater-than-optimal-scaled-depth explosions only produce proximal ejecta that contains material derived from the fallback of previous explosions over the explosion site. Fully confined explosions result in mixing in the subsurface (Graettinger et al. 2014), but do not move materials from depth to the ejecta ring. Shallow explosions are required to eject material out of the crater, so material originally located below the explosion can only be incorporated into fallback and ejecta through multiple explosions that drive the material upward until it is shallow enough to be available to subsequent explosions. The componentry of an individual ejecta deposit is dependent on the previous explosion configurations (crater and scaled depth) and sequence. Therefore, deeply derived lithic fragments are not reflective of the explosion depth that generated that specific deposit.

5.2 Implications for natural volcanic explosion deposits

The facies described from these experiments contain many important features that would be present at maar-diatremes and other volcanic craters produced by discrete subsurface explosions (Table 1). Observations of ejection and emplacement processes enable the construction of hypothetical stratigraphic columns for natural ejecta deposits, and here we focus on maar-diatremes (and their tephra rings (Fig. 7).

An eruption sequence dominated by shallower-than-optimal-scaled-depth explosions would likely produce a small tephra ring dominated by proximal ballistic fall deposits, occasional large proximal blocks, with numerous layers of bedded ash fall and isolated distal blocks (no medial blanket). A maar tephra ring that contains tuff breccias that form a pronounced proximal ring, and a thin landscape-mantling medial facies, associated with numerous large blocks within

proximal and medial facies, interbedded with occasional ash fall and density current deposits may be indicative of an optimal scaled depth explosion-dominated eruption. In this case, the tuff breccias are inferred to be the result of deposition from ballistic curtains from well-formed jets (Fig. 1a). For an eruption dominated by greater-than-optimal-scaled-depth explosions, the anticipated deposits would form a topographically subdued ring composed of deposits emplaced by fine-grained, dilute density currents that fill in the topographic variations produced by interbedded proximal wedges of breccias and tuff breccias.

The experimental observations of ejecta facies, composition and distribution reveal a dependence not only on the scaled depth of the explosion, but also the geometry of the crater system and preceding explosion sequence. All of the examples discussed here are simplified to assume the explosion location varies only in the vertical direction. Horizontal variations in explosion sites result in more-complicated distributions of facies even if scaled depth remains constant. Variation in explosion location would result in proximal facies being emplaced immediately above medial facies of previous explosions, or conversely the emplacement of medial deposits over proximal facies without changing scaled depth. Additionally, the variation of explosion location could result in inclined explosion jets, which can influence the distribution of clasts by increasing the distance an individual jet can transport material in a limited direction, while emplacing a large mass of material on the opposite side of the crater (Valentine et al. 2015). Such inclined jets in nature can result in "lateral blast" pyroclastic density currents (e.g. Lube et al. 2014). Further discussion of the influence of vent migration on ejecta distribution will be the subject of future publications.

Additionally, several mechanisms can modify a crater rim at such volcanoes, including: (1) slumping of crater walls, particularly if a crater floor subsides, which was observed at our experiments (Moore 1985; White and Ross 2011; Rottas and Houghton 2012); (2) shock-wave erosion from strong explosions; (3) destabilization and deformation due to heavy ballistic block bombardment (Gaffney et al. 1981); and (4) remobilization and deposition of material on unstable slopes by pyroclastic density currents. Such processes would result in the partial destruction and redistribution of proximal facies from deposit sequences. The complexities discussed here indicate that many lines of evidence are needed in order to relate a given feature in a maar deposit to the explosion conditions, and those observations from one or two sites cannot provide sufficient information. Instead, more comprehensive study of facies associations and their lateral distributions is needed to begin to reconstruct the explosion conditions that occurred during an eruptive sequence.

6. Conclusions

Buried-explosion experiments were used to investigate the spatial and volumetric distribution of extra-crater ejecta resulting from a range of scaled depths with and without a crater present. The multiple explosion experiments provide a reasonable analog for the formation of maar-diatreme extra-crater deposits, while explosions through undisturbed ground are more similar to military blast experiments and impact cratering. Established volcanic conduits and hydrothermal systems may also experience individual explosions, but the pre-explosion conditions are more complex than the primary blast experiments here, and thus should be compared to the multi-blast systems in which crater geometry and previous disruption have a significant effect on the explosions under investigation. The experiments use one well-constrained explosion mechanism and consequently, the variations in depositional facies distribution are the result of conditions independent of that mechanism. Thus, the experiments reveal influences on the distribution of deposits from an explosion in a debris-filled vent system that should be considered when interpreting deposits in addition to other influences. The distribution of facies from twenty-eight explosions presented here reflects a dependence on scaled depth and presence of crater. They provide a tool to reconstruct the conditions in which an explosion occurred from maar-diatreme (tephra ring) deposits. As the bulk of deposits within a tephra ring will be the result of explosions through a pre-existing crater, the facies distributions will reflect a dominant influence of the confining crater. The identification of depositional facies and the frequency of explosions at various scaled depths are important as they correlate with specific hazards. Explosions that occur at scaled depths <0.004 m/J$^{1/3}$ produce small volumes of ejecta with wide dispersal. The largest volumes of ejecta for a given explosion magnitude are produced at optimal-scaled-depth conditions (Fig. 2). This volume is distributed widely, forming a broad apron of medial ejecta. As scaled depth decreases, the volume contribution to medial ejecta decreases, and instead the bulk of the deposit is emplaced in the proximal region. However, these low-scaled-depth explosions can eject individual particles over great distances and present a hazard at distances of 20 times the crater radius.

We emphasize that the differences in distribution and character of deposits as described here are due only to the effects of scaled depth and the existence of a pre-existing crater on explosion dynamics. They do not reflect fundamental differences in phreatomagmatic or other explosion processes or the degree of magma fragmentation, which is commonly assumed by geologists when faced with variable deposit facies in volcanic ejecta or a tephra ring. In the case of maar-diatreme volcanoes especially, it is important to

keep in mind that the tephra-ring deposits are affected by a combination of explosion and magma fragmentation processes that are 'filtered' by the effects of scaled depth and crater geometry; much and in many cases most, of the record of a maar-diatreme-forming eruption is preserved underground the in the diatreme, not just in the tephra ring.

7. Acknowledgments

This work was funded by the University at Buffalo 3E fund and the National Science Foundation (EAR 1420455 to GAV). JDLW's participation was funded by the NZ Ministry of Business, Innovation and Employment via subcontract to GNS Science. Additional contributions from J. Taddeucci, D. Bowman, J. Lees and E. Macorps are gratefully acknowledged. Practical assistance was kindly provided by B. Catalano, P. Johnson, D. Klingensmith, J. Krippner, T. Macomber, S. Morealli, P. Moretti, E. Panza, D.S.C. Ruth, R. Wagner, M. Williams, and J. Wilczak. We thank Gerardo Carrasco-Nuñez and Michael Ort for their helpful reviews of the manuscript.

8. References

Andrews RG, White JDL, Dürig T, Zimanowski B (2014) Discrete blasts in granular material yield two-stage process of cavitation and granular fountaining. Geophysical Research Letters 41:422-428

Breard ECP, Lube G, Cronin SJ, Fitzgerald R, Kennedy B, Scheu B, Montanaaro C, White JDL, Tost M, Procter JN, Moebis A (2014) Using the spatial distribution and lithology of ballistic blocks to interpret the eruption sequence and dynamics: August 6, 2012 Upper Te Marri eruption, New Zealand. Journal of Volcanology and Geothermal Research 286:373-386.

Carey RJ, Manga M, Degruyter W, Swanson D, Houghton BF, Orr TR, Patrick MR (2012) Externally triggered renewed bubble nucleation in basaltic magma: The 12 October 2008 eruption at Halema'uma'u Overlook vent, Kilauea, Hawai'i, USA. Journal of Geophysical Research 117

Carrasco-Núñez G, Ort MH, Romero C (2007) Evolution and hydrological conditions of a maar volcano (Atexcac crater, Eastern Mexico). Journal of Volcanology and Geothermal Research 159:179-197

Gaffney ES (1981) Slumping and ejecta sliding accompanying some 10-ton cratering events. Geophysical Research Letters 8(12):1207-1210

Goto A, Taniguchi H (2001) Effects of explosion energy and depth to the formation of blast wave and crater: Field explosion experiment for the understanding of volcanic explosion. Geophysical Research Letters 28:4287-4290

Graettinger AH, Valentine GA, Sonder I, Ross P-S, White JDL, Taddeucci J (2014) Maar-diatreme geometry and deposits: subsurface blast experiments with variable explosion depth. Geochemistry, Geophysics, Geosystems 15:740-764.

Gurioli L, Harris AJL, Colo L, Bernard J, Favalli M, Ripepe M, Andronico D (2013) Classification, landing distribution and associated flight parameters for a bomb field emplaced during a single major explosion at Stromboli, Italy. Geology 41:559-562

Harris AJL, Ripepe M, Hughes EA (2012) Detailed analysis of particle launch velocities, size distributions and gas densities during normal explosions at Stromboli. Journal of Volcanology and Geothermal Research 231-232:109-131

Houghton BF, Swanson D, Carey RJ, Rausch J, Sutton AJ (2011) Pigeonholing pyroclasts: Insights from the 19 March 2008 explosive eruption of Kilauea volcano. Geology 39:263-266

Housen KR, Schmidt RM, Holsapple KA (1983) Crater ejecta scaling laws:Fundamental forms based on dimensional analysis. Journal of Geophysical Research: Solid Earth 88: 2485-2490

Jordan SC, Cas RAF, Hayman PC (2013) The origin of a large (>3 km) maar volcano by coalescence of multiple shallow craters: Lake Purrumbete maar, southeastern Australia Journal of Volcanology and Geothermal Research 254:5-22

Kilgour G, Manville V, Della Pasqua F, Graettinger A, Hodgson KA, Jolly GE (2010) The 25 September 2007 eruption of Moutn Ruapehu, New Zealand: Directed Ballistics, sursteyan jets, and ice-slurry lahars. Journal of Volcanology and Geothermal Research 191:1-14

Klawonn M, Houghton BF, Swanson D, Fagents SA, Wessel P, Wolfe C (2014) From field data to volumes: constraining uncertainties in pyroclastic eruption parameters. Bulletin of Volcanology 76:869

Lorenz V (1986) On the growth of maars and diatremes and its relevance to the formation of tuff rings. Bulletin of Volcanology 48:265-274

Mattox T, Mangan M (1997) Littoral hydrovolcanic explosions: a case study of lava-seawater interaction at Kilauea volcano Journal of Volcanology and Geothermal Research 75:1-17

Melosh HJ (1989) Impact Cratering. A Geologic Process. Clarendon Press. , Oxford

Moore JG (1985) Structure and eruptive mechansims at Surtsey Volcano, Iceland. Geol Mag 122: 649-661.

Ohba T, Taniguchi H, Oshima H, Yoshida M, Goto A (2002) Effect of explosion energy and depth on the nature of explosion cloud. A field experimental study Journal of Volcanology and Geothermal Research 115:33-42

Ort MH, Carrasco-Núñez G (2009) Lateral vent migration during phreatomagmatic and magmatic eruptions at Tecuitlapa Maar, east-central Mexico. Journal of Volcanology and Geothermal Research 181:67-77

Ripepe M, Rossi M, Saccorotti G (1993) Image processing of explosive activity at Stromboli. Journal of Volcanology and Geothermal Research 54:335-351

Ross P-S, White JDL, Zimanowski B, Büttner R (2008)a Multiphase flow above explosion sites in debris-filled volcanic vents: Insights from analogue experiments. Journal of Volcanology and Geothermal Research 178:104-112

Ross P-S, White JDL, Zimanowski B, Büttner R (2008)b Rapid injection of particles and gas into non-fluidized granular material, and some volcanological implications Bulletin of Volcanology 70:1151-1168

Ross P-S, White JDL, Valentine GA, Taddeucci J, Sonder I, Andrews R (2013) Experimental birth of a maar-diatreme volcano. Journal of Volcanology and Geothermal Research 260:1-12

Rottas KM, Houghton BF (2012) Structure stratigraphy and eruption dynamics of a young tuff ring: Hanauma Bay, O'ahu, Hawai'i Bulletin of Volcanology 74:1683-1697

Self S, Kienle J, Huot J-P (1980) Ukinrek Maars, Alaska, II. Deposits and formations of the 1977 craters. Journal of Volcanology and Geothermal Research 7:39-65

Taddeucci J, Valentine GA, Sonder I, White JDL, Ross P-S, Scarlato P (2013) The effect of pre-existing crater on the initial development of explosive volcanic eruptions: An experimental investigation. Geophysical Research Letters 40:507-510

Valentine GA, Graettinger AH, Sonder I (2014) Explosion depths for phreatomagmatic eruptions. Geochemistry, Geophysics, Geosystems 41 doi: 10.1002/2014GL060096

Valentine GA, Graettinger AH, Marcops, Ross PS, White JD, Sonder I, Dohring E. (2015) Experiments with vertically- and laterally- migrating explosions with applications to the geology of phreatic and phreatomagmatic eruptive centers and diatremes. Bulletin of Volcanology. doi:10.1007/s00445-015-0901-7

Table 1: Features associated with extra-crater deposits for explosions at different scaled depths.			
	<OSD	OSD	>OSD
Large Blocks	Proximal only	Proximal and medial	no
Ballistic distal	Common	Yes	No
Medial blanket	Thin	Thick	Thin to none
Steep proximal ring	High for some explosions, v. low in others (seems to be related to recharge of fallback?)	Moderate	High
Ash fall	Common	Common	Uncommon
Dilute density current deposit	Little	Some	Abundant
Total volume	Medium	Large	Small
Proximal slope (Median values from experiments, likely dependent on material type)	15-17 degrees	18-20 degrees	13-15 degrees
Slump scars in proximal	Few (explosion excavation of proximal more likely)	Common	May be common if close to threshold of confinement
Examples	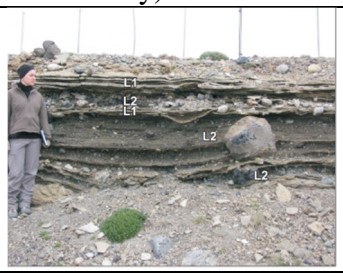		
	Tito Maar, Argentina	Lunar Crater, NV, USA	Colli Albani, Italy

Online Resources

Online Resource 1 (video): Video of experiment 2013aP2B2 showing typical ballistic curtain transport (i.e. Figure 1a). This explosion occurred at a less than optimal scaled depth (0.0028 $m/J^{1/3}$) through a pre-existing crater where the scaled depth remained constant relative to the previous explosion (i.e. Figure 5). The curtain expands away from the explosion source progressively depositing material at its base radially away from the explosion source. In these experiments the curtain produces poorly sorted proximal ejecta, a medial ejecta blanket and isolated distal clasts. The initial dark material in the jet is composed predominantly of gases from the explosion and assumed to contain minimal fine particles.

Online Resource 2 (video): Video of experiment 2013bP4B2 showing a dilute density current produced by the expulsion of fine material laterally during jet collapse into a crater (i.e. Figure 1b). This explosion occurred at greater than optimal scaled depth (0.006 $m/J^{1/3}$) through an existing crater where the scaled depth increased relative to the previous explosion (i.e. Figure 5). The density currents produced by these experiments did not produce measurable deposits, but natural volcanic explosions likely produce appreciable deposits (e.g. maar and hydrothermal explosion tephra rings).

Online Resource 3 (Table): Summary table of experimental data used in this study including explosion, crater and ejecta characterizations. The experiments are labeled by year, session (if multiple experiments were conducted in the same year), and pad number (i.e. YYYYaP#). A pad is the location of multiple explosions within the artificial stratigraphy. Previously published results and experimental descriptions can be found in Graettinger et al. (2014) for 2013a and Valentine et al. (2015) for 2014. 2013b results were previously unpublished and 2012 data did not allow for ejecta volume calculations. Primary explosions are highlighted in grey, all other explosions occurred within a pre-existing crater.

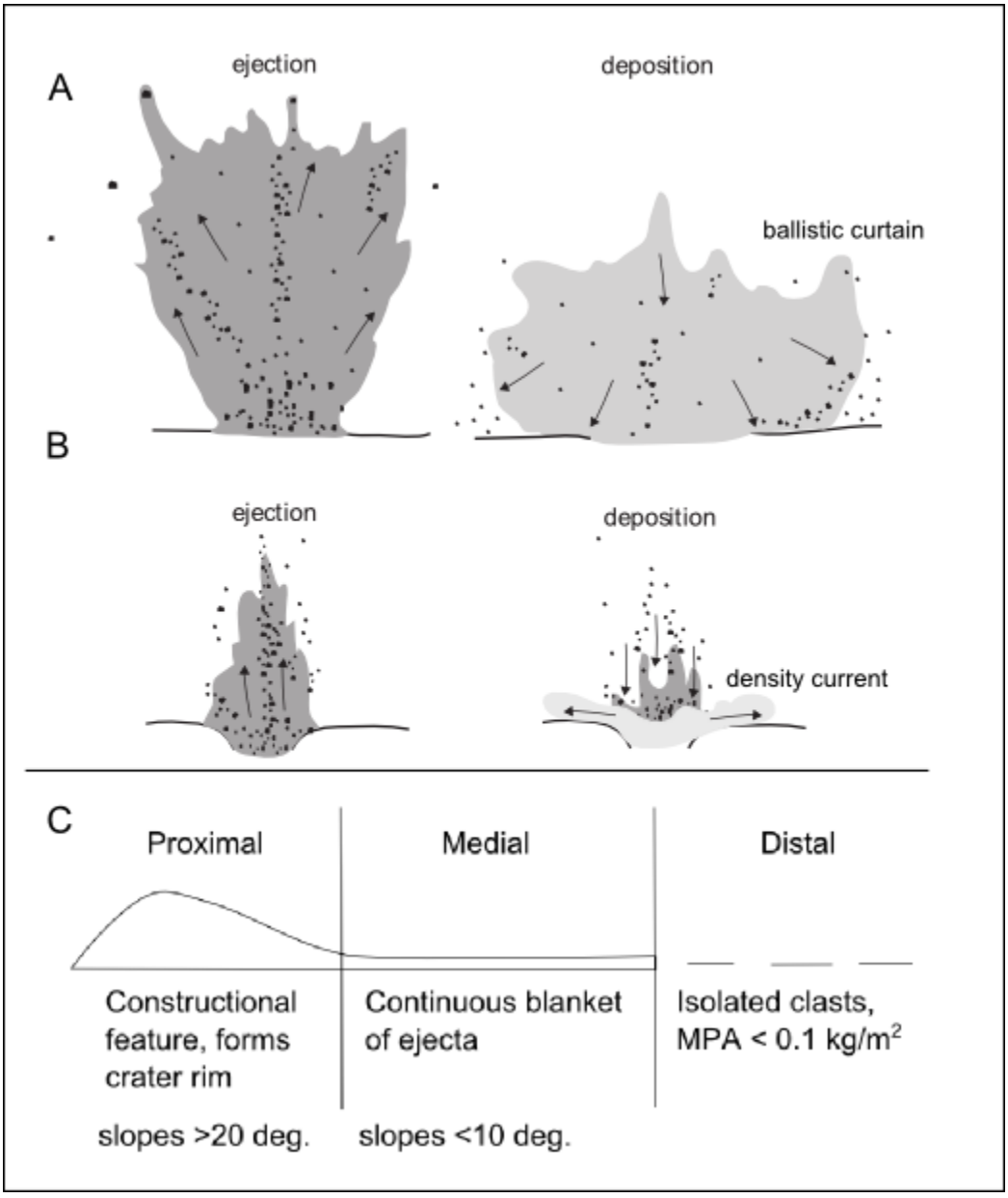

Fig. 1 Relationship between pad conditions and jet shape. A) Undisturbed pads produce wide jets that deposit material by collapsing outward as a ballistic curtain. B) Jets formed through craters or at depths greater than optimal scaled depth are more vertically focused and dominated by vertical collapse. The collapse can expel fine material producing a lateral component of deposition, similar to base surges (adapted from Graettinger et al. 2014). C) Zones of extra-crater deposition: proximal, medial and distal.

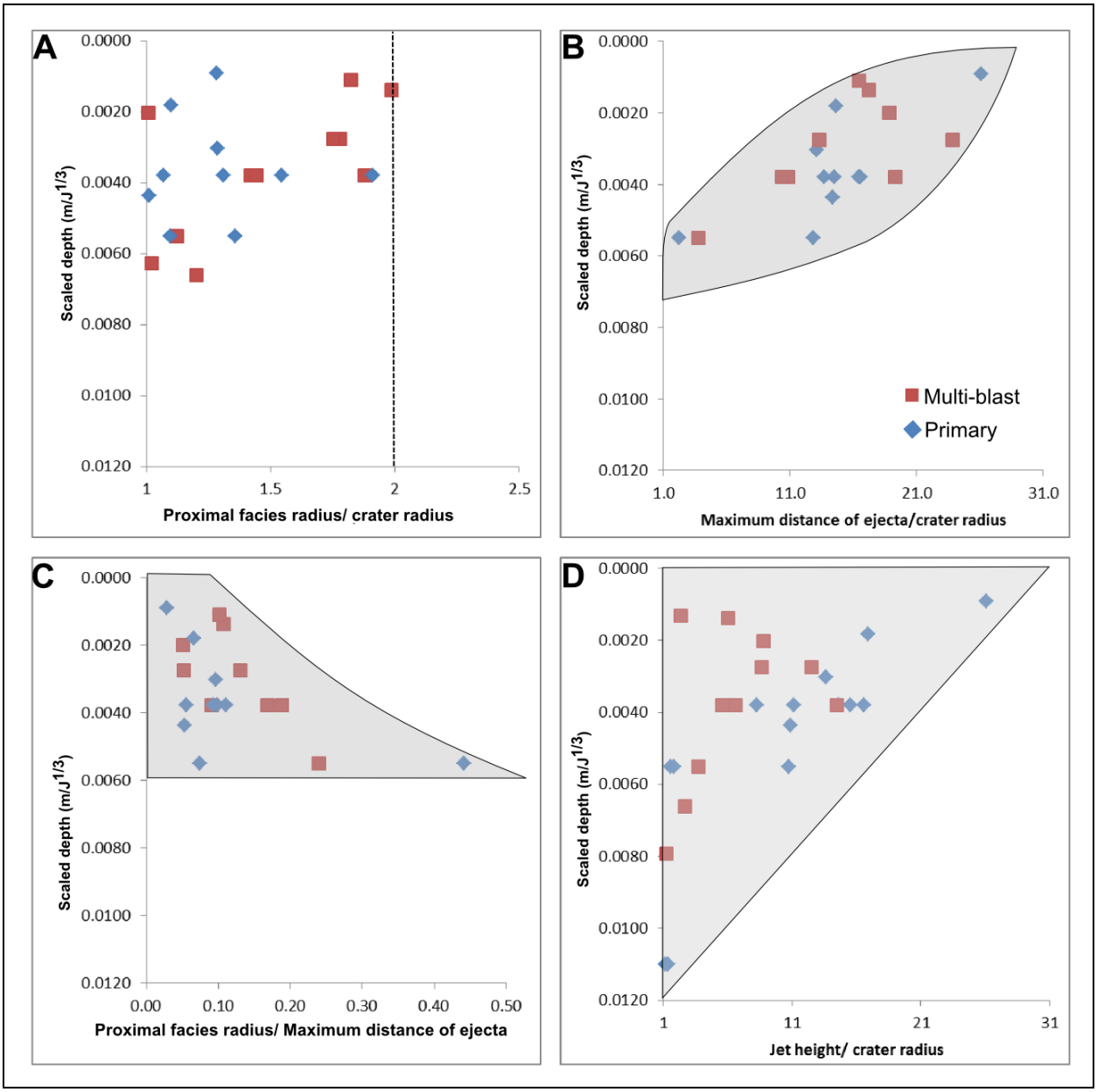

Fig. 2 Relationship between distance of ejecta distribution and scaled depth. Grey regions highlight envelopes where experimental data occurred. Trends reflect maximum values observed. A) The radius of the proximal ejecta is not sensitive to scaled depth and varies between 1 and 2 m from the explosion center. B) The maximum distance that ejecta reaches for a given explosion increases with decreasing scaled depth. C) Proximal deposits cover a greater percent of the total areal extent of ejecta with decreasing scaled depth. D) Jet height increases with decreasing scaled depth (includes >OSD data points from Graettinger et al. 2014) and is likely the control on maximum ejecta distribution. Very shallow <OSD explosions through craters have lower jet heights in part due to the travel distance through the crater.

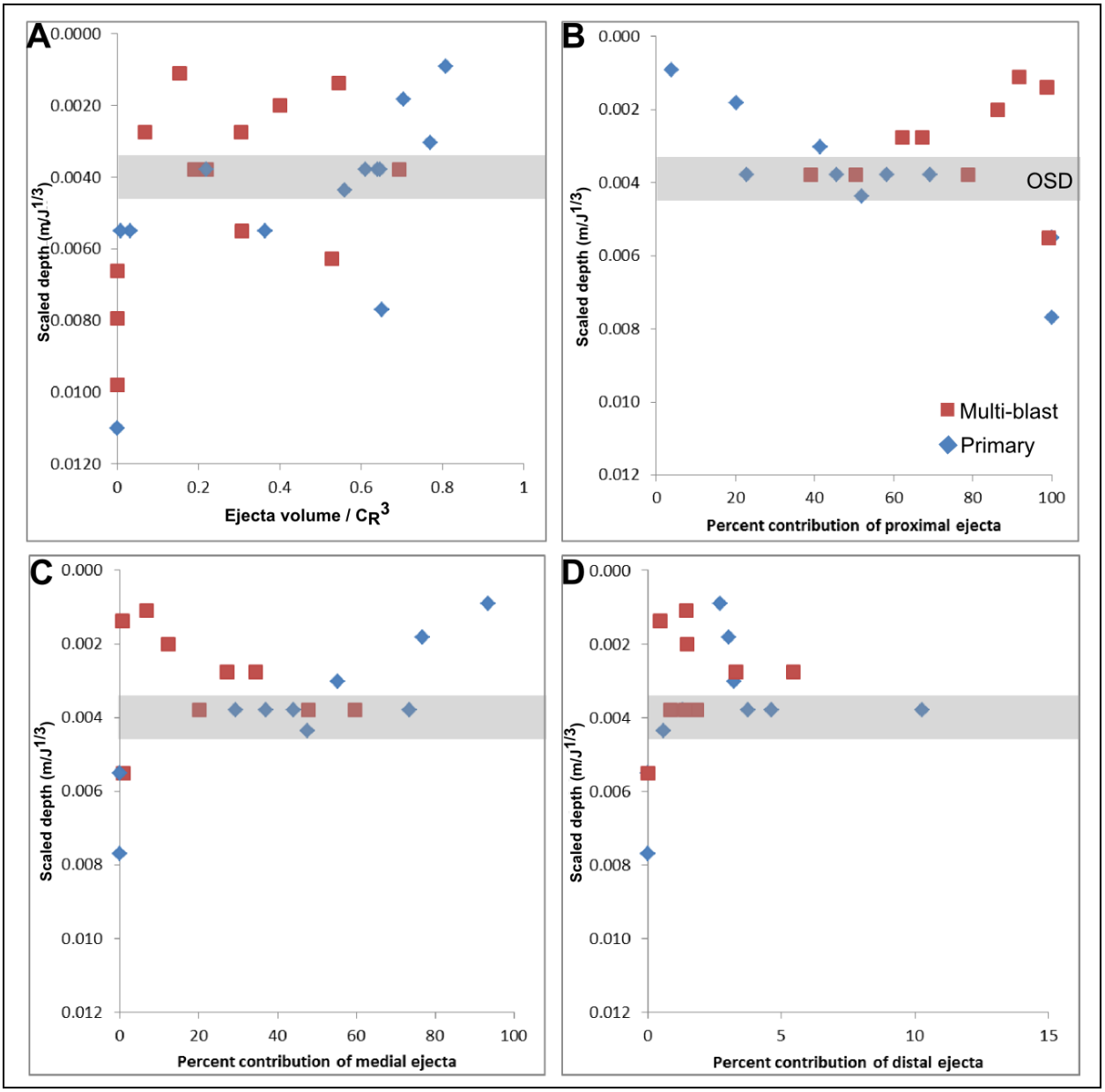

Fig. 3 Relationship between ejecta volume and scaled depth. Shaded region shows optimal scaled depth ~ 0.004 m/J$^{1/3}$ (OSD) which corresponds to the condition that produces the largest crater diameter and ejecta volume for a given energy as defined empirically. Raw volumes are included in the Online Resource 3. A) Absolute ejecta volume for both multi-blast and primary explosion systems by scaled depth. B-D) Percent volume contribution of ejecta by facies vs. scaled depth not including examples of no ejecta. B) Contribution of proximal ejecta for multi-blast and primary systems by scaled depth. C) Medial ejecta contribution for multi-blast and primary systems by scaled depth. D) Percent contribution of distal for multi-blast and primary systems by scaled depth. Note the changes in scale.

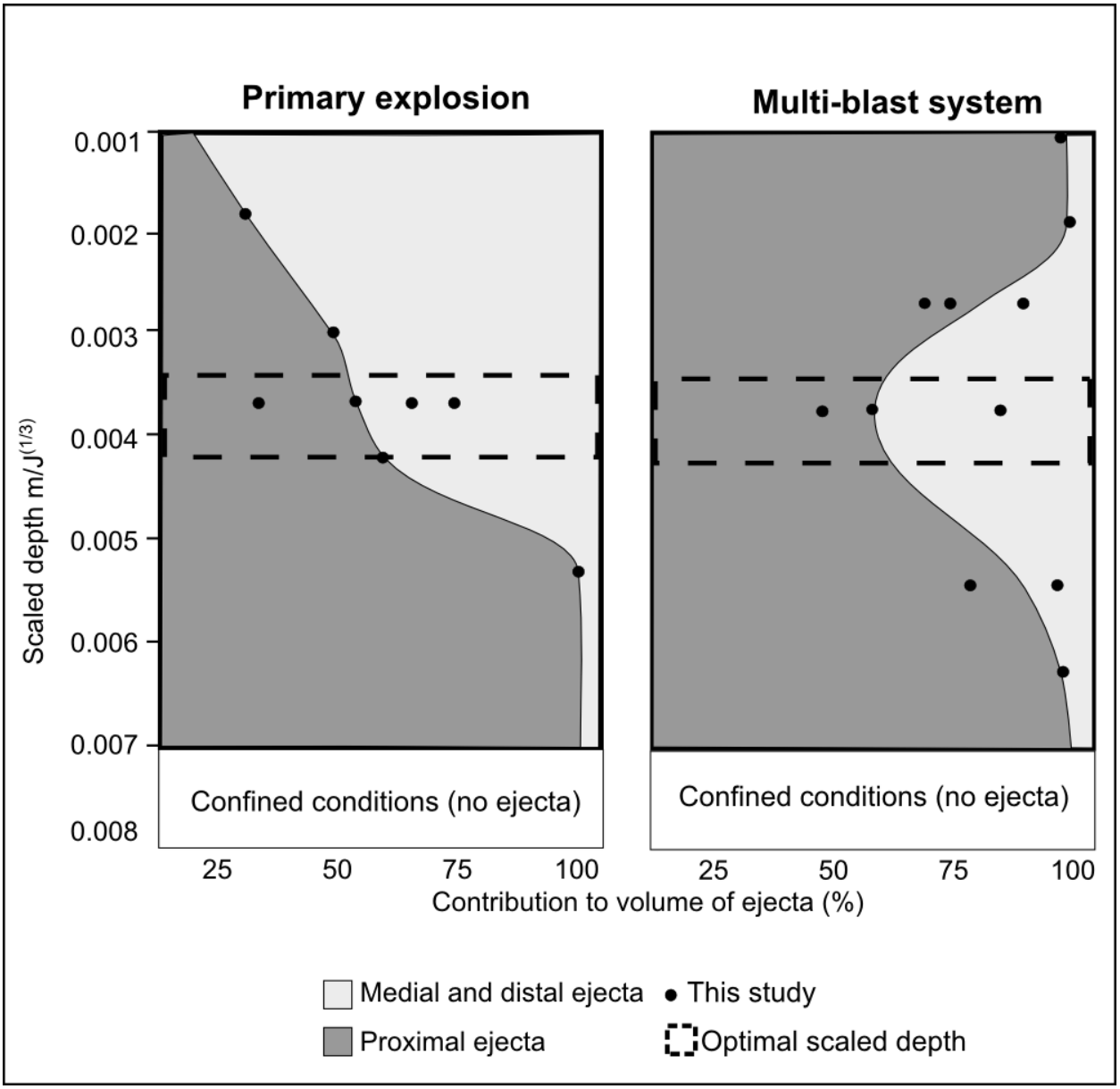

Fig. 4 Distribution of ejecta from a discrete explosion between zones (proximal, medial and distal) expressed in volume contribution (percent) compared with scaled depth. In single blast systems (primary), where there are no crater effects, the proportion of medial-distal ejecta increases with decreasing scaled depth (for scaled depths less than ~0.0055 $m/J^{1/3}$). However, if a crater is present, only explosions near the optimal scaled depth will produce appreciable medial and distal ejecta, due to the focusing effect of the crater. Distal ejecta volume proportion is insensitive to scaled depth and is here lumped with medial ejecta.

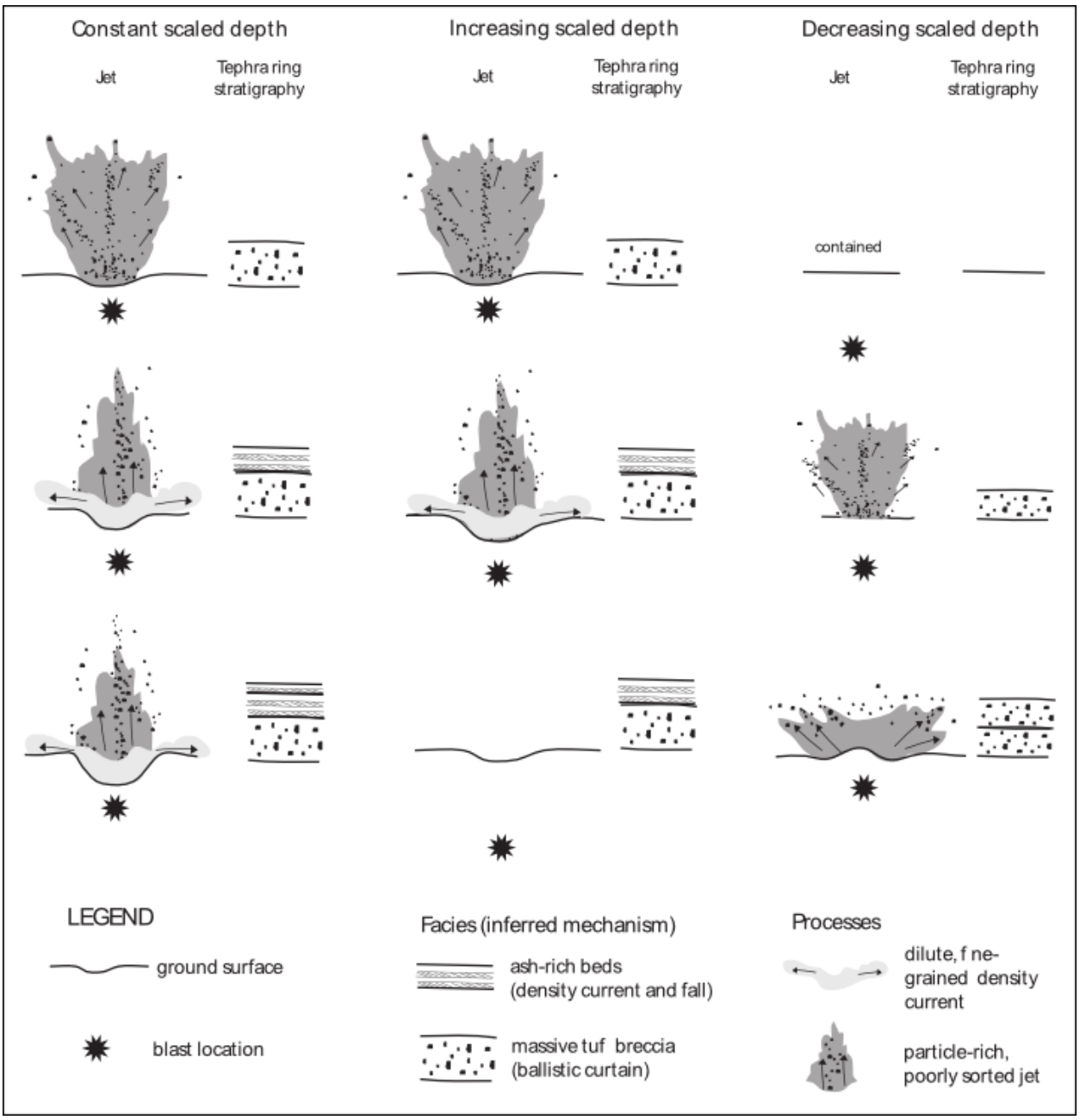

Fig. 5 Schematic relating jet shape and anticipated extra crater stratigraphy in multiple explosion systems where the scaled depth is constant, increases, or decreases. When scaled depth is constant (explosion size and depth relative to crater bottom remain constant, but depth relative to original ground surface increases) the crater focuses the jet and results in decreasing overall volumes of coarse ejecta and the potential occurrence of fine-grained dilute density current deposits. Progressively increasing scaled depth results in an overall decrease in ejecta volume to the point where the explosion is confined and no ejecta are produced. A progressive decrease in scaled depth will result in an increase in ejecta volume and in the grain size of ejecta deposits and low occurrence of fine-grained dilute density currents as the jet is larger than the previous crater and therefore does not exhibit significant focusing.

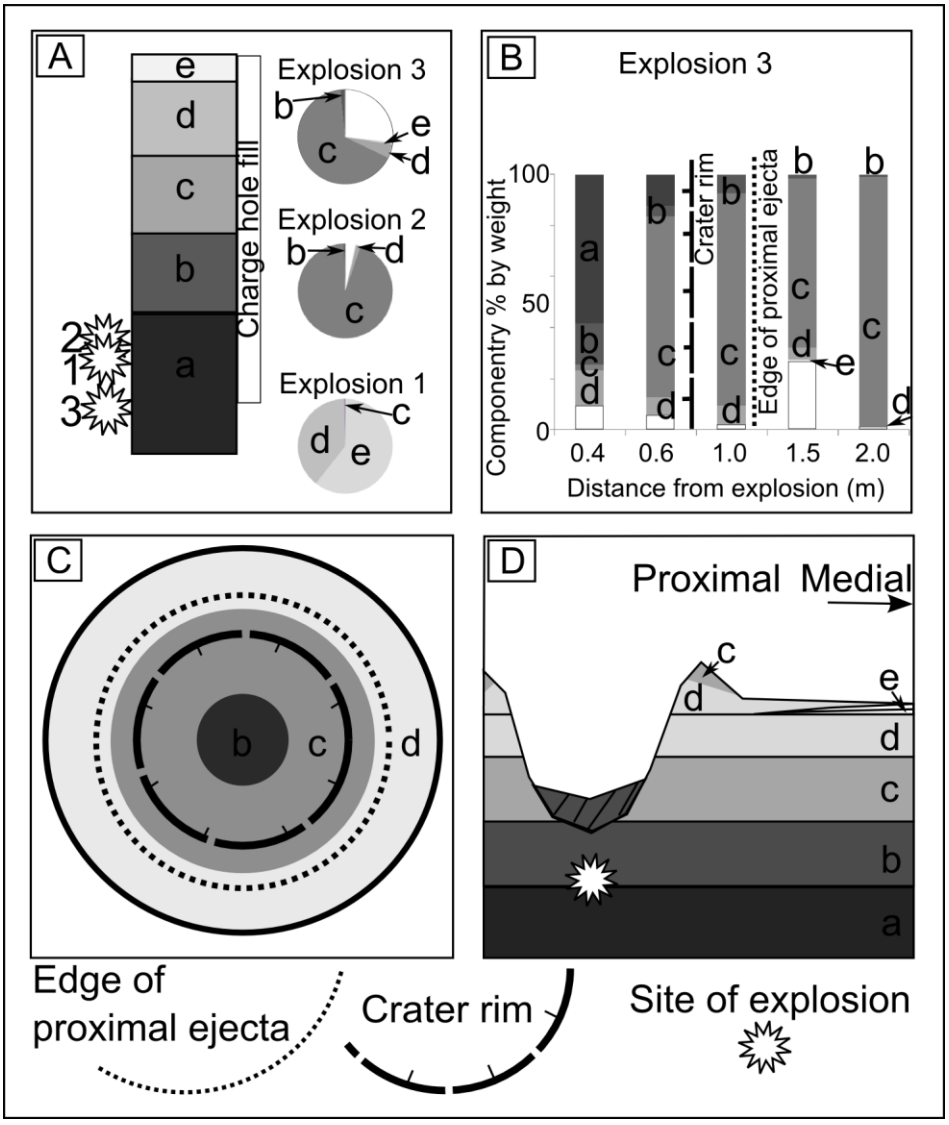

Fig. 6 Figure 6 Componentry distribution evolves as a result of multiple explosions and the presence of a crater. A) Experimental ejecta from 2013aPad3 evolution (pie charts) at a location 1.5 m from the crater (first sample box) for three explosions in a sequence denoted next to the vertical column of host stratigraphy. Early explosions are dominated by shallow material with increasing abundance of deep materials and charge hole fill. B) From the same example the ejecta from Explosion 3 with distance from the crater center. In crater componentry was only available for the final blast in the sequence. C) Idealized map view of the occurrence of material from depth from a single explosion relative to the crater rim and proximal ejecta ring (adapted from Graettinger et al. 2014). D) Cross-section of the idealized crater in C.

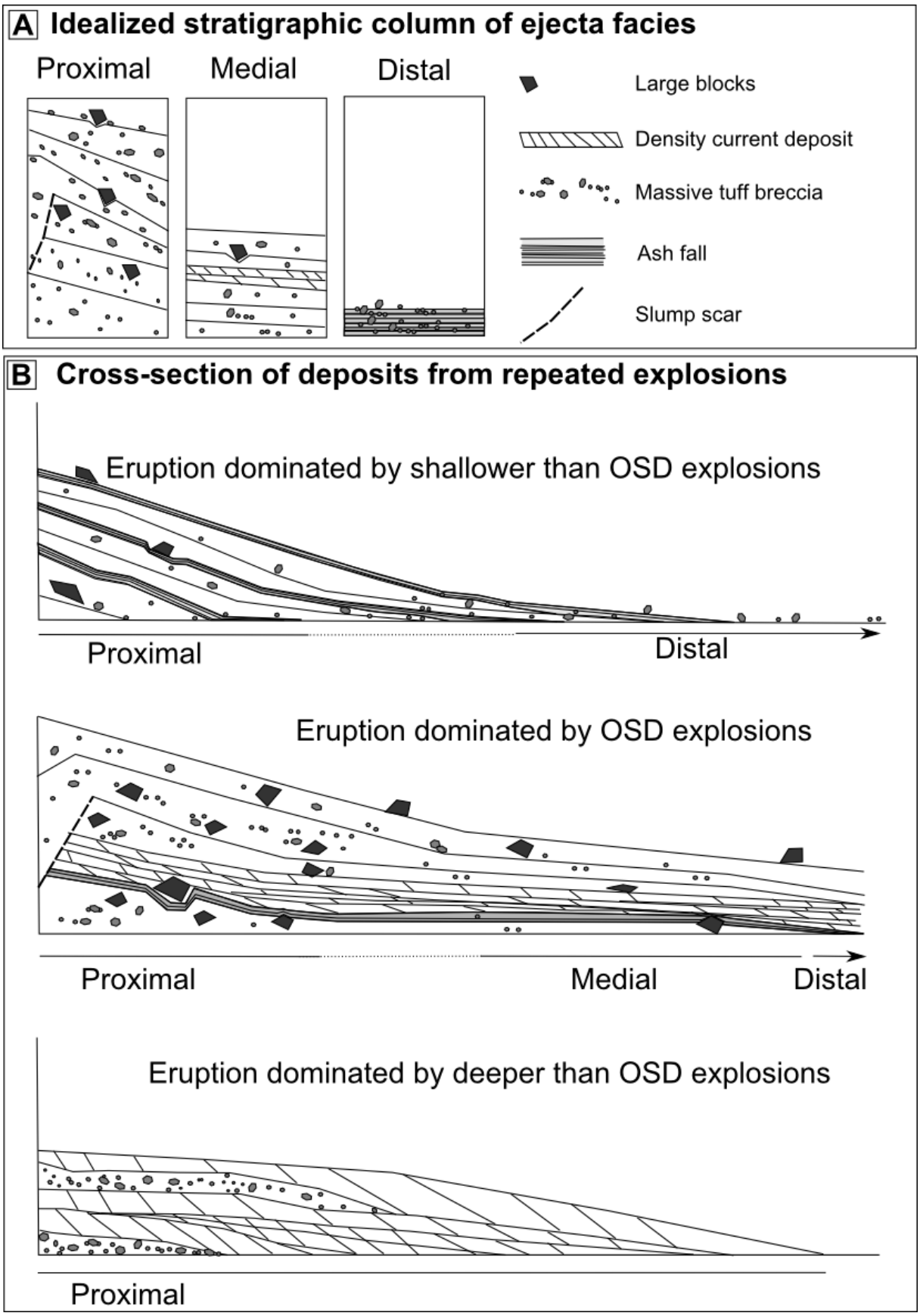
A Idealized stratigraphic column of ejecta facies
Proximal
Medial
Distal
Large blocks
Density current deposit
Massive tuff breccia
Ash fall
Slump scar
B Cross-section of deposits from repeated explosions
Eruption dominated by shallower than OSD explosions
Proximal
Distal
Eruption dominated by OSD explosions
Proximal
Medial
Distal
Eruption dominated by deeper than OSD explosions
Proximal

Fig. 7 Idealized sections of facies and facies sequences for maar-diatreme volcanoes based on explosion experiments. A) Proximal medial and distal ejecta facies are defined by experimental results with added features inferred from observations of additional experiments and crater stability. B) Idealized cross-sections are proposed for eruptions dominated by a range of scaled depth explosions.